Available online at www.sciencedirect.com
SCIENCE DIRECT®
Journal of Sound and Vibration 284 (2005) 379–392
JOURNAL OF SOUND AND VIBRATION
www.elsevier.com/locate/jsvi

Application of the R-function method to nonlinear vibrations of thin plates of arbitrary shape

Lidia Kurpa[a], Galina Pilgun[a], Eduard Ventsel[b,*]

[a]*Department of Applied Mathematics, National Technical University "Kharkov Polytechnic Institute", 21 Frunze str., 61002 Kharkov, Ukraine*

[b]*Department of Engineering Science & Mechanics, The Pennsylvania State University, 205 A Earth & Engineering Sciences Building, University Park, PA 16802-1401, USA*

Received 29 December 2003; accepted 17 June 2004
Available online 11 November 2004

Abstract

In this paper free large-amplitude flexural vibrations of thin plates with various planforms and boundary conditions are studied by the R-function method. This method is based on the joint application of the R-function theory and variational methods. The main feature of the R-function theory is the possibility to present all geometric information given in the boundary value problem in analytical form, which allows one to seek a solution in the form of some formula called the solution structure. A method of constructing the solution structures for the given nonlinear vibration plate bending problems is developed. Numerical examples of large-amplitude flexural vibrations of thin plates with arbitrary shapes and boundary conditions for illustrating the aforementioned R-function method and comparison against the other methods are made to demonstrate its merits and advantages.

1. Introduction

Geometrically nonlinear vibration analysis of thin plates is of primary importance in structural mechanics. It is well known that there are considerable mathematical difficulties associated with the complexity of mathematical formulation of the corresponding boundary value problem

*Corresponding author. Tel.: +1-814-865-4523; fax: +1-814-863-7967.
E-mail address: Ventsel@psu.edu (E. Ventsel).

0022-460X/$ - see front matter © 2004 Elsevier Ltd. All rights reserved.
doi:10.1016/j.jsv.2004.06.012

(BVP), which is governed by a system of partial nonlinear differential equations with the prescribed boundary conditions. The geometrically nonlinear vibration analysis of thin plates with various boundary conditions has been analyzed by many researchers [1–15]. In 1996, M. Sathyamoorthy had presented a comprehensive and excellent review in the field [2]. It is known that the analytical form of the solution to this class of problems may be obtained for some simple cases of plan forms and boundary conditions of the plates involved [3–5]. Therefore, some numerical methods are applied in solving nonlinear vibration problems, such as Galerkin and Ritz methods [6–8], asymptotic [9] and the method of averages [10], various perturbation techniques [11] and others. The most widely used numerical methods for the nonlinear vibration analysis are the finite element method (FEM) [12–15] and the boundary element method (BEM) [16,17]. However, in spite of the versatility of the FEM and BEM, the numerical results for the given nonlinear BVP for vibrating plates of complex planforms and various boundary conditions were reported only in few works [11,12,18].

In this paper, the R-function method (RFM) based on the joint application of variational methods and the R-function theory [19,20] and developed for the free linear vibration analysis of thin orthotropic plates in Ref. [21], is extended to the geometrically nonlinear vibration analysis of thin plates of arbitrary shape with various boundary conditions.

2. Problem statement

Consider a thin, isotropic plate of constant thickness of surface Ω and boundary $\partial\Omega$. The geometrically nonlinear dynamic analysis of thin plates is based on the governing von Karman-type nonlinear partial differential equations of motion [22]. These equations for large-amplitude vibrating thin plates are of the form [23].

$$\frac{\partial}{\partial x}\left[B\left(\varepsilon_x+\upsilon\varepsilon_y\right)\right]+\frac{\partial}{\partial y}\left[B\frac{1-\upsilon}{2}\varepsilon_{xy}\right]-\rho h\frac{\partial^2 u}{\partial t^2}=0,$$

$$\frac{\partial}{\partial x}\left[B\frac{1-\upsilon}{2}\varepsilon_{xy}\right]+\frac{\partial}{\partial y}\left[B\left(\varepsilon_y+\upsilon\varepsilon_x\right)\right]-\rho h\frac{\partial^2 v}{\partial t^2}=0, \tag{1}$$

$$\frac{\partial^2}{\partial x^2}\left[D(\chi_x+\upsilon\chi_y)\right]+2\frac{\partial^2}{\partial x\,\partial y}\left[D(1-\upsilon)\chi_{xy}\right]+\frac{\partial^2}{\partial y^2}\left[D(\chi_y+\upsilon\chi_x)\right]-\rho h\frac{\partial^2 w}{\partial t^2}=0,$$

where $B=Eh/\left(1-\upsilon^2\right)$ and $D=Eh^3/\left[12\left(1-\upsilon^2\right)\right]$ are the extensional and flexural rigidities, respectively, for an isotropic plate of uniform thickness h; E and υ are the Young modulus and the Poisson ratio, respectively, ρ is the mass density. The strain–displacement relations are of the form [23]

$$\varepsilon_x=\frac{\partial u}{\partial x}+\frac{1}{2}\left(\frac{\partial w}{\partial x}\right)^2,\quad \varepsilon_y=\frac{\partial v}{\partial y}+\frac{1}{2}\left(\frac{\partial w}{\partial y}\right)^2,\quad \varepsilon_{xy}=\frac{\partial u}{\partial y}+\frac{\partial v}{\partial x}+\frac{\partial w}{\partial x}\frac{\partial w}{\partial y},$$
$$\chi_x=-\frac{\partial^2 w}{\partial x^2},\quad \chi_y=-\frac{\partial^2 w}{\partial y^2},\quad \chi_{xy}=-2\frac{\partial^2 w}{\partial x\partial y}, \tag{2}$$

where ε_x, ε_y, and $\varepsilon_{x,y}$ are in-plane strains components at points of the plate middle surface, and χ_x, χ_y, and χ_{xy} are the flexural and twisting curvatures, respectively, u, v, and w are displacements in the x, y, z directions, respectively.

The system of differential equations (1) must be complemented with initial and boundary conditions. The four boundary conditions are prescribed along the boundary $\partial\Omega = \bigcup_{i=1}^{M} \partial\Omega_i$ as follows:

(a) Clamped edge $\partial\Omega_1$:

$$u = 0, \quad v = 0, \quad w = \frac{\partial w}{\partial n} = 0. \tag{3}$$

(b) Simply supported edge $\partial\Omega_2$, assuming that the displacements of points on the boundary are neglected

$$u = 0, \quad v = 0, \quad w = 0, \quad M_n = -D\left(\frac{\partial^2 u}{\partial n^2} + \upsilon \frac{\partial^2 u}{\partial s^2}\right) = 0, \tag{4}$$

where M_n is the normal bending moment, n is the outward normal to the boundary component $\partial\Omega_2$ and s denotes the arc length measured along the boundary.

3. The method of solution

For solving the given vibration problem, Hamilton's principle may be used in the form [24]

$$\Lambda = \int_{t_0}^{t_1} (U_s - T)\ \mathrm{d}t, \tag{5}$$

where U_S and T are the strain and kinetic energies, respectively. The corresponding expressions for these energies are given by [24]

$$U_s = \frac{1}{2}\int_{\Omega} \left\{ B\left[\varepsilon_x^2 + \varepsilon_y^2 + 2\upsilon\varepsilon_x\varepsilon_y + \frac{1-\upsilon}{2}\varepsilon_{xy}^2\right] + D\left[\chi_x^2 + \chi_y^2 + 2\upsilon\chi_x\chi_y + \frac{1-\upsilon}{2}\chi_{xy}^2\right] \right\} \mathrm{d}\Omega,$$

$$T = \frac{\rho h}{2}\int_{\Omega} \left[\left(\frac{\partial w}{\partial t}\right)^2 + \left(\frac{\partial u}{\partial t}\right)^2 + \left(\frac{\partial v}{\partial t}\right)^2 \right] \mathrm{d}\Omega, \tag{6}$$

For harmonic vibrations, displacements u, v, and w can be presented as

$$u(x,y,t) = U(x,y)\sin\lambda t, \quad v(x,y,t) = V(x,y)\sin\lambda t, \quad w(x,y,t) = W(x,y)\sin\lambda t, \tag{7}$$

where λ is the natural frequency of vibrations.

Using Eqs. (2) and (7), we can express the functional (6) in terms of u,v, and w. Integrating over the interval equal to the period of vibration, i.e. $0 \leqslant t \leqslant 2\pi/\lambda$, and taking the expressions (6) into

account, brings the functional (5) to the following form:

$$\Lambda = \frac{\pi}{2\lambda}\left[\int_{\Omega}\left\{B\left[\left(\frac{\partial U}{\partial x}+\frac{\partial V}{\partial y}\right)^2+2(\upsilon-1)\left(\frac{\partial U}{\partial x}\frac{\partial V}{\partial y}-\frac{1}{4}\left(\frac{\partial U}{\partial y}+\frac{\partial V}{\partial x}\right)^2\right)\right]\right.$$
$$\left.+D\left[\left(\frac{\partial^2 W}{\partial x^2}+\frac{\partial^2 W}{\partial y^2}\right)^2-(1-\upsilon)\left(\frac{\partial^2 W}{\partial x^2}+\frac{\partial^2 W}{\partial y^2}-2\left(\frac{\partial^2 W}{\partial x\partial y}\right)^2\right)\right]\right\}\mathrm{d}\Omega$$
$$+\frac{3B}{4}\int_{\Omega}\left[\frac{1}{2}\left(\frac{\partial w}{\partial x}\right)^2+\frac{1}{2}\left(\frac{\partial w}{\partial y}\right)^2\right]^2\mathrm{d}\Omega-\lambda^2\rho h\int_{\Omega}\left(W^2+U^2+V^2\right)\mathrm{d}\Omega\Bigg]. \tag{8}$$

In the above expression, the first integral represents the strain energy due to the linear deformation of the plate, while the second integral represents the strain energy due to the nonlinear straining of the plate. The third integral is the kinetic energy of the plate assuming the harmonic vibrations.

It is known from the theory of variational methods that the solution of the governing equations of the given nonlinear BVP with the boundary conditions (3) and (4) is equivalent to the problem of minimizing the functional (8) [25]. The minimization of the functional can be carried out on a set of functions satisfying only the so-called principal or kinematic boundary conditions (3) and the first three conditions (4), while the fourth condition (4), as well as the boundary conditions for the free edge of the plate (not presented above), are natural for the functional (8). The latter will be satisfied automatically in the minimization of the functional.

The minimization of functional (8) will be carried out by the Ritz method. Before proceeding further with this procedure, let us notice that the above functional is not a quadratic function of the displacement components. Therefore, we will slightly modify this functional. Let us introduce some additional functions f_1 and f_2 as follows:

$$f_1=\frac{1}{2}\frac{\partial W}{\partial x},\quad f_2=\frac{1}{2}\frac{\partial W}{\partial y}. \tag{9}$$

Let us assume that f_1 and f_2 are known functions. Upon substitution of Eqs. (9) into functional (8) one transforms it into the quadratic functional of unknown functions U, V, and W, i.e.

$$\Lambda = \frac{\pi}{2\lambda}\left[\int_{\Omega}\left\{B\left[\left(\frac{\partial U}{\partial x}+\frac{\partial V}{\partial y}\right)^2+2(\upsilon-1)\left(\frac{\partial U}{\partial x}\frac{\partial V}{\partial y}-\frac{1}{4}\left(\frac{\partial U}{\partial y}+\frac{\partial V}{\partial x}\right)^2\right)\right]\right.$$
$$\left.+D\left[\left(\frac{\partial^2 W}{\partial x^2}+\frac{\partial^2 W}{\partial y^2}\right)^2-(1-\upsilon)\left(\frac{\partial^2 W}{\partial x^2}+\frac{\partial^2 W}{\partial y^2}-2\left(\frac{\partial^2 W}{\partial x\partial y}\right)^2\right)\right]\right\}\mathrm{d}\Omega$$
$$+\frac{3B}{4}\int_{\Omega}\left[f_1\frac{\partial w}{\partial x}+f_2\frac{\partial w}{\partial y}\right]^2\mathrm{d}\Omega-\lambda^2\rho h\int_{\Omega}(W^2+U^2+V^2)\,\mathrm{d}\Omega\Bigg]. \tag{10}$$

According to the R-function method, let us construct the solution structures for the displacement components satisfying the prescribed principal boundary conditions (3) and (4). For example, the following solution structure will satisfy the boundary conditions (3) and (4)

$$U=\omega\cdot P_1,\quad V=\omega\cdot P_2,\quad W=\omega^k\cdot P_3, \tag{11}$$

where $\omega = 0$ is the equation of the whole boundary Ω. The values of the exponent k for the function $\omega(x, y)$ in Eqs. (11) are selected depending on the type of boundary conditions involved, i.e., $k = 1$, if the plate is simply supported and $k = 2$ when the plate is clamped over the boundary. For the case of mixed boundary conditions, i.e., clamped–simply supported edges of the plate, the solution structure is defined as

$$U = \omega P_1, \quad V = \omega P_2, \quad W = \omega\omega_1 P_3, \tag{12}$$

where $\omega_1 = 0$ is the equation of the clamped part of the boundary $\partial\Omega_1$; P_1, P_2, and P_3 are some indefinite components given by

$$P_1(x,y) = \sum_{i=1}^{N_1} a_i\varphi_i(x,y), \quad P_2(x,y) = \sum_{i=N_1+1}^{N_2} a_i\varphi_i(x,y), \quad P_3(x,y) = \sum_{i=N_2+1}^{N_3} a_i\psi_i(x,y), \tag{13}$$

where $\{\varphi_i(x,y)\}$, $\{\phi_i(x,y)\}$, and $\{\psi_i(x,y)\}$ are known elements (coordinate functions) of some functional space containing the above indefinite components and forming some complete sequences in this space. For example, we may select the system of algebraic polynomials, Chebushev or Legendre polynomials, trigonometric polynomials or some finite functions (spines, atomic functions, etc.) as $\{\varphi_i(x,y)\}$, $\{\phi_i(x,y)\}$ and $\{\psi_i(x,y)\}$. In the present case, the algebraic polynomials are chosen as complete sets of the above functions. The undetermined coefficients a_i $(i = 1, 2, \ldots N_3)$ are evaluated from the conditions of minimizing functional (10), which result in the following system of equations

$$\frac{\partial \Lambda}{\partial a_i} = 0 \quad (i = 1, \ldots, N_3). \tag{14}$$

For a construction of the solution structure it is necessary to select the functions $\omega(x, y)$ and $\omega_1(x, y)$ in Eqs. (12) in such a way that the following conditions will be satisfied:

$$\omega(x,y) = 0, \forall(x,y) \in \partial\Omega; \quad \omega_1(x,y) = 0, \forall(x,y) \in \partial\Omega; \quad \omega(x,y) > 0, \forall(x,y) \in \Omega.$$

The fact that the function $\omega(x, y)$ vanishes only at points of the boundary is highly essential, since otherwise some "unnecessary conditions" may be imposed on the solution. As a result of that, the chosen functions $P_i, i = 1, 2, 3$ will not be able to provide a sufficient accuracy of the solution, i.e., the solution structures will not be complete.

The problem of minimization of the functional (10) for the given nonlinear BVP is solved by using the following iterative procedure. In the first step of the iterative process, the above-introduced functions (9) are set equal to zero, i.e., $f_1 = f_2 = 0$. Then, minimizing the functional (10), one can obtain the solution for the linear frequencies λ_m and the corresponding eigenfunctions W_m. The latter are scaled up by some given amplitude of vibration W_m^* at some fixed point of the plate $M_0(\xi, \eta)$. As a rule, $M_0(\xi, \eta)$ is the point where the corresponding eigenfunction reaches its maximum value. Having determined the eigenfunction that corresponds to the chosen frequency, one can determine functions f_1 and f_2 for the following steps of the iterative process.

Thus, by knowing the functions f_1 and f_2, one can minimize functional (10) by the iterative technique, iteration is continued until a modified Euclidean norm based on the difference between the eigenfunctions, obtained for the two adjacent iterations, will not exceed the given value of

accuracy ε, i.e.

$$\sum_{j=N_2+1}^{N_3}\left(\frac{a_j^{(r)}-a_j^{(r-1)}}{a_j^{(r-1)}}\right)^2<\varepsilon,$$

where r is the number of iteration, $a_j^{(r)}, a_j^{(r-1)}$ are the coefficients that determine eigenfunctions W_m on r and $r-1$ iterations, respectively, from the formulas

$$W_m^{(r)}(x,y)=\sum_{j=N_2+1}^{N_3}a_{jm}^{(r)}w_j,\quad W_m^{(r-1)}(x,y)=\sum_{j=N_2+1}^{N_3}a_{jm}^{(r-1)}w_j,\quad m=1,2,\ldots,(N_3-N_2+1).$$

3. Numerical results

The proposed method for nonlinear vibrations of thin plates has been incorporated into a software system POLE–RL based on a general RFM formulation for various problems of solid mechanics [20]. Some results of numerical investigations, obtained with this software system to illustrate the performance of the method, its relative accuracy, and overall effectiveness are presented below. Testing of the proposed method was carried out for plates of simple and complex geometry having simply supported and clamped edges, as well as mixed boundary conditions. The parameters of investigated plates are: thickness $h/a=0.01$, Poisson's ratio $\upsilon=0.3$. The accuracy of the iterative calculation was assigned to be $\varepsilon=0.0001$. The integration was implemented numerically by using 12-point Gaussian quadrature.

3.1. Example 1

Let us consider a square plate with the following boundary conditions: (1) the plate is clamped along $x=\pm a$ and simply supported along $y=\pm a$ (CSCS); (2) the plate is clamped along $x=-a, y=-a$ and simply supported along $x=a, y=a$ (CCSS); (3) the plate is clamped along $x=\pm a, y=a$ and simply supported along $y=-a$ (CCCS); (4) the plate is clamped along $y=-a$ and simply supported along $x=\pm a, y=-a$ (CSSS).

The presented numerical results below were obtained for each type of the above-indicated boundary conditions by using the solution structures (12). Table 1 presents the fundamental frequency period ratios T/T_L, where T is nonlinear and T_L are linear periods, respectively, for the given isotropic square plate. All of the numerical results given in Table 1 have been obtained by retaining in expansions (12):

(1) 70 coordinate functions for the CSCS boundary conditions.This corresponds to 10th degrees algebraic polynomials approximating U and V and 12th degree polynomial approximating W with regard to the symmetry of the plate and boundary conditions.
(2) 208 coordinate functions for the CCSS boundary conditions. This corresponds to 9th degrees algebraic polynomials approximating U and V and 11th degree polynomial approximating W with no symmetry taken into account.

Table 1
Fundamental frequencies periods ratios T/T_L of square plates

Type of boundary conditions		$\omega_L = \lambda_L a^2\sqrt{\frac{\rho}{D}}$	T/T_L at W^*/h				
			0.2	0.4	0.6	0.8	1
CSCS	RFM	28.951 28.948 [26]	0.9934	0.9743	0.9446	0.9073	0.8651
	[14]	–	0.9904	0.9633	0.9227	0.8739	0.8214
CCSS	RFM	27.056 27.208 [26]	0.9819	0.9653	0.9272	0.8815	0.8326
	[14]	–	0.9863	0.9487	0.8953	0.8349	0.7741
CSSS	RFM	23.647 23.648 [26]	0.9896	0.9603	0.9170	0.8656	0.8110
	[14]	–	0.9848	0.9431	0.8845	0.8190	0.7538
CCCS	RFM	31.826 31.875 [26]	0.9934	0.9756	0.9477	0.9126	0.8732
	[14]	–	0.9906	0.9642	0.9248	0.8776	0.8271

Note: W^*/H the nondimensional mazimum amplitude of the deflection.

(3) 94 coordinate functions for the CCCS and CSSS boundary conditions. This corresponds to 9th degrees algebraic polynomials approximating U and V and 11th degrees polynomial approximating W, taking the symmetry of the given plate and boundary conditions about the y- axis into account.

The number of the above-indicated coordinate functions has been established by analyzing numerically the stabilization of the T/T_L ratios convergence in the iterative process.Further increases in the number of the coordinate functions did not affect the accuracy of the solution

To examine the accuracy of the numerical results obtained by the RFM, they are compared with those obtained in Refs. [14, 26]. Table 1 also demonstrates a good agreement between the above-mentioned numerical results. The percentage error did not exceed 0.05%.

As part of numerical testing procedure, the fundamental frequency period ratios T/T_L were calculated with the assumption that the first derivatives in Eqs. (2) are negligible; thus, the error introduced by the use of the simplified expressions for the midsurface strains of the form

$$\varepsilon_x = f_1\frac{\partial W}{\partial x}, \quad \varepsilon_x = f_2\frac{\partial W}{\partial y}, \quad \varepsilon_{xy} = f_1\frac{\partial W}{\partial y} + f_2\frac{\partial W}{\partial x} \tag{15}$$

was evaluated. The results of this investigation are shown in Figs. 1(a) and (b). These results have shown that substituting Eqs. (15) into functional (6), the values of ratios T/T_L approach those obtained in Ref. [14]. The maximum deviations of the test results with those of Ref. [14] in this case do not exceed 0.009%.

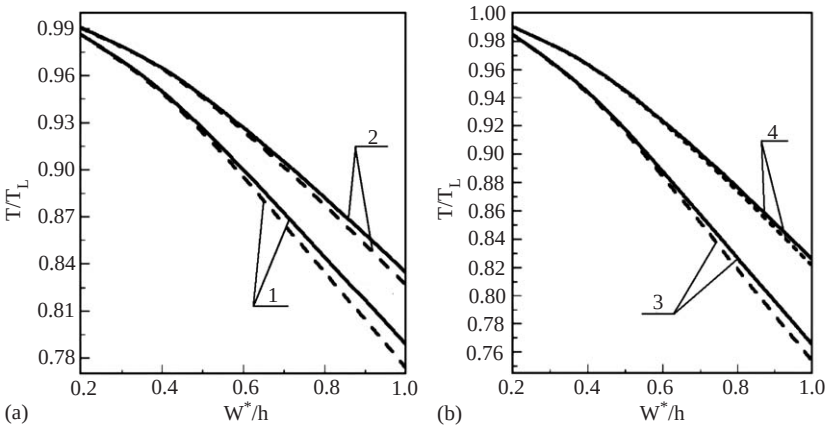

Fig. 1. The fundamental frequency period ratios, T/T_L, obtained by using the proposed procedure (solid lines) and taken from Ref. [14] (dashed lines) for the square plate with the following boundary conditions: (a) the curves 1 and 2 correspond to the CCCS (the edges $x = \pm a$ and $y = a$ are clamped and the edge $y = -a$ is simply supported) and to the CCSS (the edges $x = -a$ and $y = -a$ are clamped and the edges $x = a$ and $y = a$ are simply supported) boundary conditions, respectively; (b) the curves 3 and 4 correspond to the CSCS (the edges $x = \pm a$ are clamped and the edges $y = \pm a$ are simply supported) and to the CSSS (the edge $y = -a$ is clamped and the edges $y = \pm a$, $y = -a$ are simply supported) boundary conditions, respectively.

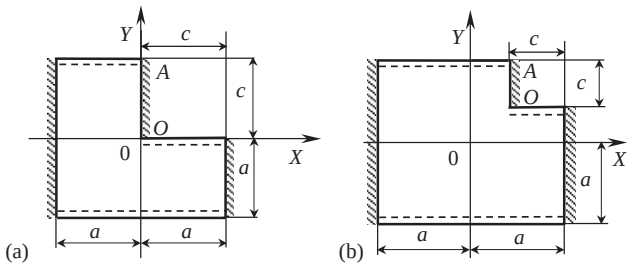

Fig. 2. An angular plate with mixed boundary conditions having the cut depth equal: (a) $c/a = 1$; (b) $0 \leqslant c/a \leqslant 1$.

3.2. Example 2

Consider a plate having a cut with $c/a = 1$ as shown in Fig. 2(a). The plate has mixed boundary conditions: the shaded parts of the boundary are clamped, while the dashed lines indicate simply supported parts of the boundary. The nonlinear vibration analysis of such a plate was carried out in Ref. [13].

In this case, the functions $\omega(x, y)$ and $\omega_1(x, y)$ entering into structure (12) may be represented in the form:

$$\omega = (F_1 \wedge_0 F_2) \wedge_0 (F_3 \vee_0 F_4), \tag{16}$$

$$\omega' = F_2 \wedge_0 \varpi, \quad \text{where } \varpi = \sqrt{F_3 \cdot F_3 \vee_0 F_5}. \tag{17}$$

In these expressions, $F_1=(a^2-x^2)/2a\geqslant 0$, $F_2=(a^2-y^2)/2a\geqslant 0$, $F_3=(-x)=0$, $F_4=(-y)\geqslant 0$, $F_5=\left(x^2+\left(y-a/2\right)^2-\left(a/2\right)^2\right)\geqslant 0$, and $\wedge_0,\vee_0$ R- conjunction and R- disjunction, respectively, determined as [19]

$$x\wedge_0 y=x+y-\sqrt{x^2+y^2},\quad x\vee_0 y=x+y+\sqrt{x^2+y^2}.$$

A construction of the clamped edge boundary $\omega_1(x,y)$ for the plate shown in Fig. 2a, without application of the R- functions causes considerable difficulties because it requires writing the equation of the line segment OA belonging to the straight line $x=0$ [18,21]. Using the R-functions, the above equation of the line segment OA may be represented by Eqs. (17). At that time, the function $\varpi(x,y)$ is equal to zero only at points of this segment.

The values of the fundamental frequency ratios λ/λ_L of the plate (Fig. 2a) are presented in Table 2 depending on the nondimensional maximum amplitude of the deflection, W^*/h, for the plate shown in Fig. 2.

The numerical results in this table are given for the two variants of the conducted calculations: with the use of the simplified kinematic relations (15) [RFM$^{(a)}$] and with the use of the general von Karman kinematic relations (2) [RFM$^{(b)}$]. As it follows from the comparison of these results with those reported in Ref. [13], the incorporation of the first derivatives of the in-plane displacements associated with stretching of the plate, $\partial U/\partial x$ and $\partial V/\partial y$, results in reduction of the corresponding values of the frequencies. The calculated discrepancies of the compared numerical results varies: in the variant of calculation (a) from $\approx 0.001\%$ to $\approx 0.0203\%$; in the variant of calculation (a) from $\approx 0.0049\%$ to $\approx 0.0332\%$.

For the vibration analysis of the plate shown in Fig. 2(a), the total number of coordinate functions in the expansions (13) was equal to 75, which corresponds to 4th degree algebraic polynomials approximating U and V and 8th degree polynomials approximating W. The above number has been ascertained by an investigation of the stability of the convergence of the ratios λ/λ_L in the iterative process.

3.3. Example 3

Let the depth of the cut for the plate of Fig. 2(b) vary from $c=a$ to 0. We will analyze below the influence of this parameter on the fundamental frequency ratios λ/λ_L. Notice that if $c\neq 0$, F_3, F_4 and F_5 should be presented in expressions (16) and (17) in the form

$$F_3=(c-x)\geqslant 0,\quad F_4=(c-y)\geqslant 0,\quad F_5=\left((x-c)^2+\left(y-\frac{a-c}{2}-\right)^2-\left(\frac{a-c}{2}\right)^2\right)\geqslant 0.$$

Table 2
Fundamental frequency ratios of plate of Fig. 2

	W^*/h						
	0.2	0.4	0.6	0.8	1	1.2	1.4
[13]	1.015	1.056	1.119	1.196	1.284	1.377	1.477
RFM$^{(a)}$	1.014	1.053	1.114	1.193	1.287	1.392	1.507
RFM$^{(b)}$	1.010	1.041	1.090	1.156	1.235	1.327	1.428

Expressions for F_1 and F_2 will be of the same form as those in Eqs. (16) and (17). Table 3 presents some numerical results of the investigation of influence of the cut depth c/a on frequency ratios for the plate shown in Fig. 2b. The above numerical results in this table are also depicted in Fig. 3 in terms of the cut depth c/a versus the frequency ratios for the values of the amplitudes $(W^*/h) = (0.6, 1, 1.4)$.

The deviation of the values of the frequency ratio for the investigated plate of complex form for $c/a \to 0$ from the corresponding values of λ/λ_L obtained previously for the square plate was not more than 0.0027% (for the same boundary conditions).

Table 3
Influence of the cut depth c/a on the fundamental frequency ratio λ/λ_L

	c/a	W^*/h											
		1	0.9	0.8	0.7	0.6	0.5	0.4	0.3	0.2	0.1	0.01	0
RFM	0.2	1.010	1.009	1.008	1.008	1.008	1.007	1.007	1.008	1.008	1.008	1.008	1.008
[13]		1.015	–	–	–	–	–	–	–	–	–	–	1.009
RFM	0.4	1.041	1.040	1.033	1.030	1.030	1.029	1.029	1.030	1.030	1.031	1.031	1.031
[13]		1.056	–	–	–	–	–	–	–	–	–	–	1.038
RFM	0.6	1.090	1.079	1.072	1.065	1.065	1.064	1.064	1.066	1.067	1.068	1.068	1.068
[13]		1.119	–	–	–	–	–	–	–	–	–	–	1.084
RFM	0.8	1.156	1.136	1.124	1.113	1.112	1.110	1.112	1.114	1.116	1.117	1.118	1.117
[13]		1.196	–	–	–	–	–	–	–	–	–	–	1.144
RFM	1	1.235	1.204	1.187	1.170	1.170	1.167	1.169	1.172	1.175	1.177	1.178	1.178
[13]		1.284	–	–	–	–	–	–	–	–	–	–	1.217
RFM	1.2	1.327	1.281	1.259	1.235	1.236	1.232	1.234	1.238	1.243	1.246	1.247	1.247
[13]		1.377	–	–	–	–	–	–	–	–	–	–	–
RFM	1.4	1.428	1.367	1.338	1.308	1.309	1.303	1.307	1.312	1.318	1.321	1.323	1.323
[13]		1.477	–	–	–	–	–	–	–	–	–	–	–

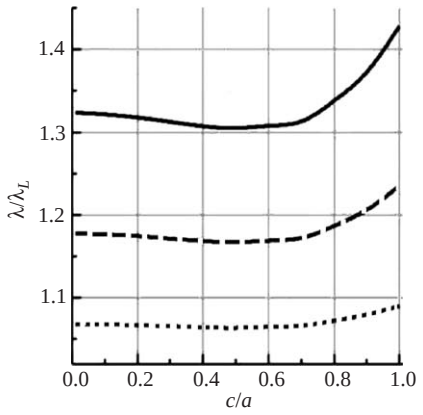

Fig. 3. The influence of the cut depth c/a on the fundamental frequencies ratio $\lambda/\lambda_L$for the three nondimensional maximum amplitudes of the deflection: $W^*/h = 1.4$ (solid line), $W^*/h = 1$ (dashed line), and $W^*/h = 0.6$ (dotted line).

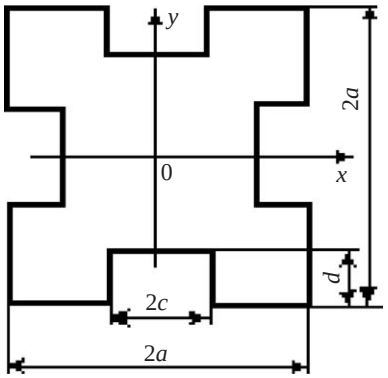

Fig. 4. Plate with four cuts.

3.4. Example 4

Consider a plate having four symmetrical cuts (see Fig. 4) with the two types of homogeneous boundary conditions along all edges: simply supported and clamped. Numerical analysis was carried out for each type of boundary conditions using the solution structure (11). The equation of the boundary component for the plate may be represented as

$$\omega = (F_1 \wedge_0 F_2) \wedge_0 ((-F_3) \vee_0 F_4) \wedge_0 (F_5 \vee_0 (-F_6)), \tag{18}$$

where $F_1 = (a^2 - y^2)/2a \geqslant 0$, $F_3 = (c^2 - y^2)/2c \geqslant 0$ and $F_5 = ((a-d)^2 - y^2)/2(a-d) \geqslant 0$ are the horizontal strips located between the straight lines $y = \pm a, y = \pm c$ and $y = \pm(a-d)$, respectively. Let $F_2 = (a^2 - x^2)/2a \geqslant 0$ be the vertical strip located between the straight lines $x = \pm a$. $F_4 = ((a-d)^2 - x^2)/2(a-d) \geqslant 0$ be the vertical strip bounded by the straight lines $x = \pm(a-d)$, and, at last, let $F_6 = (c^2 - x^2)/2c \geqslant 0$ be the vertical strip bounded by the straight lines $x \pm c$; $\wedge_0, \vee_0$ are the R- operations [19].

A comprehensive study of the vibrations for the given plate is presented in Tables 4 and 5. This study is associated with the influence of the cut depth on the ratios of higher frequencies λ/λ_L ($m = 2, n = 1$ and $m = 2, n = 2$), as well as with the dependence of the linear frequency parameter, $\Lambda_L = \lambda_L a^2 \sqrt{\rho/D}$, on the dimensionless value of the maximum amplitude W^*/h for the two above-indicated boundary conditions and is presented in Table 4.

In order to check the accuracy of the obtained numerical results, the cut depth $c \to 0$ so that the shape of the plate is approached to the square one. A comparison of the numerical results obtained by the RFM and by the FEM reported in Ref. [12-14] is presented in Table 5. This comparison demonstrates the accuracy of the proposed method.

4. Conclusion

A variational formulation with RFM and iterative procedure for solving the geometrically nonlinear free flexural vibrations of thin plates of arbitrary shape with various boundary conditions has been presented. RFM enables one to seek the solution of the given eigenvalue

Table 4
Higher frequency ratios λ/λ^L of the plate shown in Fig. 4

m	n	d/a	Λ_L	λ/λ_L at W^*/h				
				0.2	0.4	0.6	0.8	1
				Simply supported				
		0.01	52.020	1.0162	1.0635	1.1394	1.2391	1.3595
			49.396	1.0238	1.0917	1.1953	1.3255	1.4746
2	1	0.1	71.003	1.0106	1.0419	1.0928	1.1619	1.2475
		0.2	92.275	1.0096	1.0380	1.0839	1.1458	1.2224
		0.3	117.89	1.0108	10.422	1.0925	1.1605	1.2463
		0.4	154.11	1.0126	1.0545	1.1286	1.2313	1.3572
		0.01	82.897	1.0141	1.0555	1.1213	1.2079	1.3113
			79.163	1.0184	1.0713	1.1525	1.2549	1.3725
2	2	0.1	98.622	1.0108	1.0428	1.0944	1.1635	1.2474
		0.2	124.71	1.0089	1.0354	1.0783	1.1362	1.2071
		0.3	146.93	1.0082	1.0316	1.0702	1.1228	1.1879
		0.4	161.87	1.0092	1.0361	1.0788	1.1352	1.2031
				Clamped				
		0.01	73.777	1.0088	1.0349	1.0772	1.1343	1.2044
			73.558	1.0149	1/0571	1.1209	1.2007	1.2923
2	1	0.1	86.007	1.0088	1.0346	1.0765	1.1329	1.2030
		0.2	108.66	1.0093	1.0365	1.0801	1.1381	1.2087
		0.3	144.63	1.0124	1.0487	1.1075	1.1871	1.2530
		0.4	200.83	1.0115	1.0450	1.0972	1.1670	1.2578
		0.01	108.36	1.0089	1.0349	1.0769	1.1328	1.2009
			108.77	1.0136	1.0522	1.1104	1.1828	1.2653
2	2	0.1	118.59	1.0084	1.0329	1.0724	1.1250	1.1889
		0.2	143.94	1.0078	1.0307	1.0674	1.1163	1.1756
		0.3	186.64	1.0074	1.0290	1.0637	1.1103	1.1674
		0.4	237.04	1.0055	1.0218	1.0485	1.0849	1.1299

problem in the form of an analytical expression and to construct approximation sequences with the use of variational, projection, and any other methods. As a result, RFM holds the general advantages of classical analytical methods, while enabling one to solve vibration eigenvalue problems for domains of complicated plan forms.

It has been shown that the method yields rapid and convergent numerical results, which are in a good agreement with those obtained with the use of other numerical or approximate techniques. The accuracy and applicability of the RFM for the class of the geometrically nonlinear vibration plate bending problems considered in this paper has been verified successfully.

The further extension of the RFM for the dynamic analysis by considering the geometrically linear and nonlinear free and forced vibration of composite plates of an arbitrary geometry with mixed boundary conditions forms the key subject of the authors continuing research. The results of the new investigations will be reported in due course.

Table 5
The higher frequencies ratios λ/λ_L for the square plate

m	n		Λ_L	λ/λ_L at W^*/h				
				0.2	0.4	0.6	0.8	1
				Simply supported				
		[13]	–	1.0218	1.0832	1.1774	1.2973	1.4363
		[14]	–	1.0314	1.0528	1.1154	1.1979	1.2967
1	1	RFM[a]	19.740	1.0314	1.0528	1.1154	1.1979	1.2967
		[12]	19.739	1.0185	1.0716	1.1534	1.2565	1.3752
		RFM[b]	19.740	1.0185	1.0715	1.1532	1.2565	1.3756
		[13]	–	1.0300	1.1136	1.2194	1.3902	1.5600
		RFM[a]	49.349	1.0162	1.0636	1.1393	1.2392	1.3594
2	1	[12]	49.396	1.0238	1.0917	1.1953	1.3255	1.4746
		RFM[a]	49.349	1.0237	1.0913	1.1946	1.3246	1.4737
		[13]	–	1.0216	1.0833	1.1782	1.2985	1.4375
		RFM[a]	78.957	1.0131	1.0513	1.1124	1.1929	1.2895
2	2	[12]	79.163	1.0184	1.0713	1.1525	1.2549	1.3725
		RFM[b]	78.957	1.0184	1.0713	1.1526	1.2555	1.3738
				Clamped				
1	1	[12]	36.004	1.0070	1.0276	1.0607	1.1046	1.1575
		RFM[a]	35.985	1.0018	1.0081	1.0209	1.0417	1.0705
		RFM[b]	35.985	1.0070	1.0276	1.0607	1.1046	1.1576
		[12]	73.558	1.0149	1.0571	1.1209	1.2007	1.2923
2	1	RFM[a]	73.394	1.0088	1.0347	1.0767	1.1334	1.2030
		RFM[b]	73.394	1.0140	1.0542	1.1165	1.1963	1.2901
		[12]	108.77	1.0136	1.0522	1.1104	1.1828	1.2653
2	2	RFM[a]	108.22	1.0083	1.0329	1.0727	1.1262	1.1916
		RFM[b]	108.22	1.0125	1.0486	1.1052	1.1784	1.2647

References

[1] A.W. Leissa, Vibrations of plates, NASA SP-160, NASA, Washington, DC, 1969.
[2] M. Sathyamoorthy, Nonlinear vibrations of plates: an update of recent research developments a review, *Applied Mechanics Reviews* 49 (1996) s55–s62.
[3] H.N. Chu, G. Hermann, Influence of large amplitudes on free flexural vibrations of rectangular elastic plates, *Journal of Applied. Mechanics* 23 (1956) 532–540.
[4] T. Wah, Large amplitude flexural vibrations of rectangular plates, *International Journal of Mechanical Science* 5 (1963) 425–438.
[5] Mei Chuh, Finite element displacement method for large amplitude free flexural vibrations of beams and plates, *Zeitschrift für angewandte Mathematik und Mechanik* 41 (1961) 501–510.
[6] G.C. Kung, Y.H. Pao, Nonlinear flexural vibrations of a clamped circular plate, *Journal of Applied Mechanics* 39 (1972) 1050–1054.
[7] N. Yamaki, K. Otomo, M. Chiba, Nonlinear vibrations of a clamped circular plate with initial deflection and initial edge displacement, Part 1: Theory, *Journal of Sound and Vibration* 79 (1981) 23–42.
[8] C.P. Vendham, Y.C. Das, Application of Rayleigh–Ritz and Galerkin method to nonlinear vibration of plates, *Journal of Sound and Vibration* 39 (1975) 147–157.

[9] N.I. Zhinzher, V.E. Khromotov, Asymptotic method in problems of nonlinear vibration of rectangular slightly orthotropic plates, *Soviet Applied Mathematics* 20 (1984) 742–746.
[10] C.L. Huang, et al., Finite amplitude vibrations of a circular plate, *Journal of International Nonlinear Mechanics* 12 (1977) 297–306.
[11] D.W. Lobitz, D.T. Mook, A.H. Nayfeh, Nonlinear analysis of vibrations of irregular plates, *Journal of Sound and Vibration* 50 (1977) 203–217.
[12] C. Mei, R. Narayanaswami, G.V. Rao, Large amplitude free flexural vibrations of thin plates of arbitrary shape, *Computers and Structures* 10 (1979) 675–681.
[13] Y. Shi Y, C. Mei, A finite element time domain modal formulation for large amplitude free vibrations of beams and plates, *Journal of Sound and Vibration* 193 (1996) 453–464.
[14] G.V. Rao, I.S. Raju, K.K. Raju, A finite element formulation for large amplitude flexural vibrations of thin rectangular plates, *Computers and Structures* 6 (1976) 163–167.
[15] Mei Chuh, A. Kamolphan Decha-Umphai, A finite element method for nonlinear forced vibrations of rectangular plates, *AIAA Journal* 23 (1984) 1104–1110.
[16] R.S. Srinivasan, P.A. Krishnan, Application of integral equation technique to nonlinear stochastic response of rectangular plates, *Journal of the Acoustical Society of America* 88 (1990) 2277–2283.
[17] X.X. Wang, J. Qian, M.K. Huang, Boundary integral equation formulation for large amplitude nonlinear vibration of thin elastic plates, *Computer Methods in Applied Mechanics and Engineering* 86 (1991) 73–86.
[18] B. Banerjee, Large-amplitude vibrations of polygonal plates—A new approach, *Journal of Applied Mechanics* 51 (1984) 211–213.
[19] V.L. Rvachev, *Theory of R-Functions and Some of its Applications*, Nauka Dumka, Kiev, Ukraine 1982 (in Russian).
[20] V.L. Rvachev, T.I. Sheiko, R-functions in boundary value problems in mechanics, *Applied Mechanics Reviews* 48(4) (1997) 151–188.
[21] L.V. Kurpa, V.L. Rvachev, E.S. Ventsel, The R-function method for the free vibration analysis of thin orthotropic plates of arbitrary shape, *Journal of Sound and Vibration* 26 (2003) 109–122.
[22] C.Y. Chia, *Nonlinear Analysis of Plates*, McGraw-Hill, New York, 1980.
[23] A.S. Volmir, Flexible Plates and Shells, Air Force Flight Dynamics Laboratory TR 66–216 1967.
[24] M. Sathyamoorthy, *Nonlinear Analysis of Structures*, CRC Press, Boca Raton, Boston, 1997.
[25] S.G. Mikhlin, *Variational Methods in Mathematical Physics*, Pergamon Press, Oxford, 1964.
[26] P.M. Varvak, A.F. Ryabov (Eds.), *The Reference Book on the Theory of Elasticity*, Budivelnik, Kiev, Ukraine, 1971 (in Russian).